Published by IOP Publishing for Sissa Medialab

Received: *September 29, 2019*
Revised: *November 12, 2019*
Accepted: *November 25, 2019*
Published: *January 15, 2020*

21[st] International Workshop on Radiation Imaging Detectors
7–12 July 2019
Crete, Greece

Study of a small scale position-sensitive scintillator detector for γ-ray spectroscopy

Zh. Toneva,[1] S. Ivanov, G. Georgiev, V. Kozhuharov and S. Lalkovski

Department of Nuclear Engineering, Faculty of Physics,
University of Sofia "St. Kliment Ohridski", Sofia, Bulgaria

E-mail: zh.h.toneva@phys.uni-sofia.bg

Abstract: Precision measurement of the energy and direction of gamma-rays plays a key role in many fields such as medical imaging, nuclear spectroscopy, and astrophysics. In astrophysics position sensitive gamma-ray detectors are used to study diffuse and point-like sources. These space-born gamma-ray telescopes, however, are mainly based on large arrays of detectors which are expensive, complex, and take long time to build. A different approach is the use of detector with similar energy and angular resolution, but small enough to be deployed on nanosatellites.

We research a design based on monolithic scintillator and multi-pixel photo-sensor. At first we are focused on characterization of $CeBr_3$ scintillator detectors. Bench test experiments were performed with $CeBr_3$ crystal with square surfaces and thicknesses of 10 mm and 25 mm. The crystals were coupled to a single-anode PMT and the outcome compared to Geant4 simulation.

Keywords: Gamma detectors (scintillators, CZT, HPG, HgI etc); Gamma telescopes; X-ray detectors and telescopes

[1]Corresponding author.

https://doi.org/10.1088/1748-0221/15/01/C01013

Contents

1 Introduction

The gamma-ray imaging and spectroscopy technologies have wide applications in many scientific fields, such as nuclear physics and astrophysics amongst others, but also have a large impact on various socio-economic fields, such as homeland security and medical physics. Thus, the development of a new technology that can be used for detection of electromagnetic radiation in the sub-MeV and MeV energy range is of paramount interest [1]. The research and development of novel gamma-ray detectors, working in this energy range, is also of great importance for observations of transient astrophysical events and diffuse galactic sources [2]. To date, the region of low energy cosmic gamma-rays is still not well explored. Different technologies exists on the market today, which are mainly based on large scintillators or high purity germanium (HPGe) detectors. These, however, have rather poor spatial resolution and imaging capabilities. In order to improve the latter, separate detector modules built of highly pixelized CdZnTe detectors are usually used. This approach is proven to be expensive, complex, and taking long time to build. Also, in many cases additional subsystems are needed for cooling, shielding etc., which increases the mission's cost and the risk of failure. This technology is applied in the only telescope that presently observes the sky in the sub-MeV and MeV regime — INTEGRAL [3]. The mission has several subsystems, two of which are SPI and IBIS, that are used for spectroscopy and imaging, respectively. After the end of INTEGRAL mission, the future of observations in sub-MeV and MeV regime is unclear.

Indeed, future proposals for large-scale missions are being considered — ASTROGAM [4] in Europe, COMPAIR [5] and AMEGO [6] in the US but, given the typical development time, those will be ready for use (if approved) in 2030s at earliest. Possible solution to bridge the time gap between the present and future missions could come from the development of light telescopes that can be launched on state-of-the art nanosatellites. The CubeSat technology provides the means to built a cheap observatory that would be affordable by national funding agencies, research centers and universities.

As such, of particular interest for the present study is the development of a novel detector technology that can be used in space-borne telescopes, compatible with the rapidly developing nanosatellite technology. The working assumption is that a gamma-ray telescope can be realized by two detector layers, as shown in figure 1, used for measurements of energy and angle of incidence. The front layer, placed close to the “aperture” of the telescope, will be used as a scatterer. Its geometry needs to be optimal for single Compton scattering process to occur. The purpose of the second layer is to fully absorb the scattered gamma-rays. In order to reproduce the angle of incidence precisely, the two detector layers have to have good position resolutions. Given the space and power constraints of the nanosatelites, the two layer planes must be placed several tens of centimeters apart to achieve optimum spatial resolution. Fast coincidence circuits will be used to eliminate background events. Similar two-layers design was used in the past by COMPTEL [7], on board of the Compton Gamma Ray Observatory. The present approach, however, relies on the most recent developments in scintillator and photomultiplier technologies. As such, we aim to achieve better position- and energy- resolutions when compared to COMPTEL, but reducing the size of the mission.

Here, we present some preliminary results on position resolution and response function of a scintillator detectors built of $CeBr_3$ crystals coupled to multi-pixel photo-sensor or single-anode photomultiplier tube. Preliminary results from bench test experiments of a monolithic scintillator coupled to a multi-pixel photomultiplier (PMT) are presented elsewhere [8].

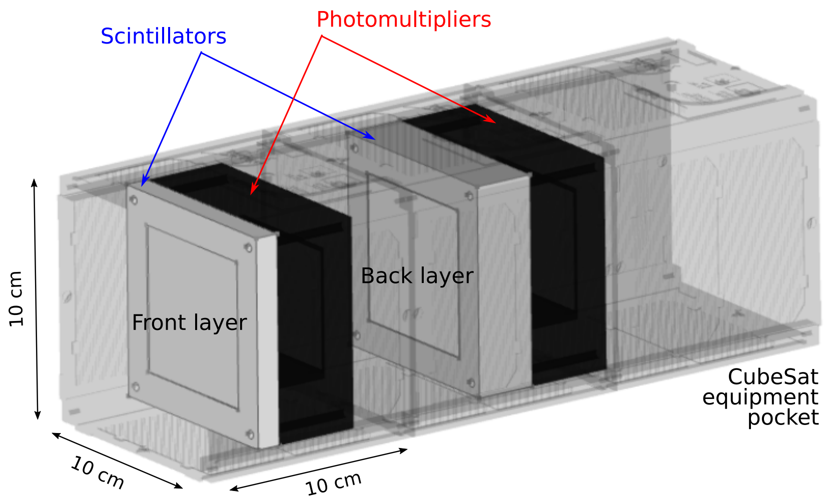

Figure 1. Prototype of a nanosatellite with Compton camera designed in our group and placed inside 3 units CubeSat modules, designed by NASA [9]. Each detector consists of monolithic scintillation crystal coupled to a multi-pixel PMT.

2 Experimental setup and measurements

Given that a single detector is expected to provide spectroscopic information and to generate images of astronomical objects, it should possess good position-, time- and energy- resolutions. In order for the telescope to match the SPI and COMPTEL performances, and given the nanosatelites constraints,

2020 JINST 15 C01013

each of the detectors has to have a position resolution better than 5 mm, energy resolution better than 5% at 662 keV, and time resolution of the order of 150 ps. These are prerequisites for precise calculation of the angle of incidence, disentanglement of different radiation sources, and generation of sharp images. In addition, the enhanced time resolution is required for background subtraction, via fast-coincidence circuits, and a real time data reduction.

2.1 Materials

This work exploits new materials that have emerged in the last decades, that are commercially available in different geometries and sizes, but not used in space-borne gamma telescopes, yet. The family of the lanthanum-halide scintillators is amongst the most exploited materials, having high light yield, good energy and time resolution. Comparative characteristics of two materials namely $CeBr_3$ and $LaBr_3$:Ce, are presented in table 1. The lower light yield of $CeBr_3$ [10], when compared to $LaBr_3$:Ce [11], results in worse energy resolution. However, a key advantage of $CeBr_3$ material is its low intrinsic activity. This would result in 25 times shorter observation time if $CeBr_3$ is used instead of $LaBr_3$:Ce detectors of the same size and geometry [10].

Preliminary results are presented for two square shaped $CeBr_3$ scintillators (51 by 51 mm^2) with thickness of 10 mm and 25 mm, respectively. These are commercially available and purchased from Scionix.

Table 1. Comparison between $CeBr_3$ and $LaBr_3$:Ce scintillator material. Energy resolution FWHM is taken for $E_\gamma = 662$ keV [10, 12], time resolutions in FWHM for $CeBr_3$ [13] and $LaBr_3$:Ce [14] is obtained for $E_\gamma = 511$ keV, and position resolution at $E_\gamma = 356$ keV [15].

	Energy resolution [%]	Time resolution [ps]	Position resolution [mm]	Light yield ph/MeV	Peak emission [nm]
$CeBr_3$	4	<210	<5.4	45 000	380
$LaBr_3$:Ce	3	<154	<8.0	63 000	370

2.2 Measurements

The $CeBr_3$ crystals were coupled to XP20D0B fast 8-dynode photomultiplier tube [16] for energy response studies. The test setup was mounted in 3D printed PLA holders. Typical PMT gain, when operated at −1000 V [17], is approximately 5.5×10^6 [16]. PMT's geometry is a round cylinder with a diameter of 51 mm. As such, the PMT surface does not exactly match the optically transparent surface of the crystal. Indeed, it was encircled in the crystal's squared surface. The signals were processed by preamplifier, amplifier [18, 19], and multi-channel analyzer [20]. The N957Demo [20] acquisition software was used to discriminate pulses, and storing in text files for off-line analysis. Gamma-ray sources (^{137}Cs, ^{22}Na and ^{241}Am) with energies from 60 keV up to 1.3 MeV were placed at the detector surface and used to study detectors response. Sample energy spectra from these measurements are presented in figure 2.

2020 JINST 15 C01013

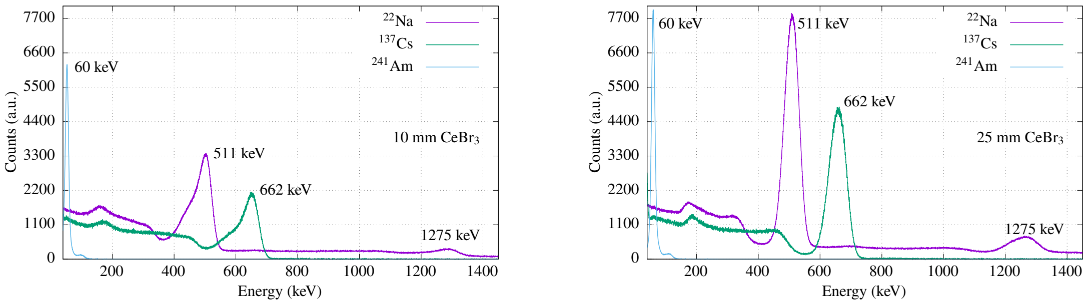

Figure 2. Recorded energy spectra of ^{137}Cs, ^{22}Na and ^{241}Am sources for 10 mm (left image) and 25 mm (right image) thick $CeBr_3$ scintillators. Due to the different source activity, the spectra were rescaled for better comparison.

2.3 Geant4 simulations

In order to simulate detectors response Geant4 simulations are being performed. Geant4 is an object-oriented C++ Monte Carlo (MC) toolkit for simulating interaction of charged particles through matter [21]. Since its version 10.0-beta, the Geant4 can model data-driven photon production from user-defined scintillators, photon transportation through arbitrarily complex detector geometries and time-resolved photon detection at the light readout device [22]. To optimize and compare the results from the measurements with those coming from Geant4, two configuration codes were developed. The first code focuses on the study of the energy resolution while the second one concentrates into the future scintillator geometry and its position resolution when coupled to a multi-anode PMT [23]. Distribution of the incident photons on the surface of the photomultiplier was recorded. Note that in both simulations the gamma-ray source and the scintillator crystals with the optical window were included. Furthermore, the simulation utilizes a point-like source with predefined gamma-ray beam, which energy, direction, angular distribution were varied in an iterative process. Figure 3 presents simulations geometry for 10 mm and 25 mm thick $CeBr_3$ scintillators. The gamma-rays and the consequent products interact in $CeBr_3$ crystals according to the FTPT_BERT library of Geant4. The scintillation at each of the interaction positions (hits) were simulated as uniform emission of 45 optical photons per 1 keV of deposited energy [10]. The simulation does not take into account the PMT quantum efficiency, the photoelectron emission and only assumes Poissonian distribution of the scintillations. In both simulations, detector geometry was imported into Geant4 through GDML [24].

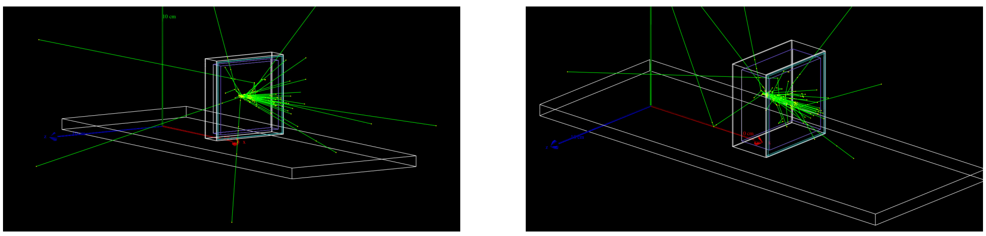

Figure 3. Geometry of Geant4 simulations for 10 mm (left image) and 25 mm (right image) $CeBr_3$.

2020 JINST 15 C01013

3 Results

3.1 Energy resolution

Energy calibrations of the experimental data were made by using a second order polynomial. Source peaks, shown in the spectra on figure 2, were fitted using χ^2 method. The energy resolution in terms of $R = \mathrm{FWHM}/E_\gamma$, as a function of the full energy peak, is shown in figure 4. The R values, measured with present set up, deviate significantly from producer's specifications. This is due to incomplete light collection on the PMT surface which is smaller when compared to the scintillator's transperant area. As seen from figure 4, the MC simulation confirms the experimental observation that, for $E_\gamma > 500$ keV, there is no significant difference in the energy resolution between the 10 mm and the 25 mm $CeBr_3$ scintillator. At lower energies, the energy resolution of the thicker crystal is much better than the resolution of the thinner crystal, which probably is due to the better light collection. This effect is not well understood. Further analysis is now carried out to resolve the issue. New equipment need to be procured in order to overcome the PMT — crystal geometrical incompatibility.

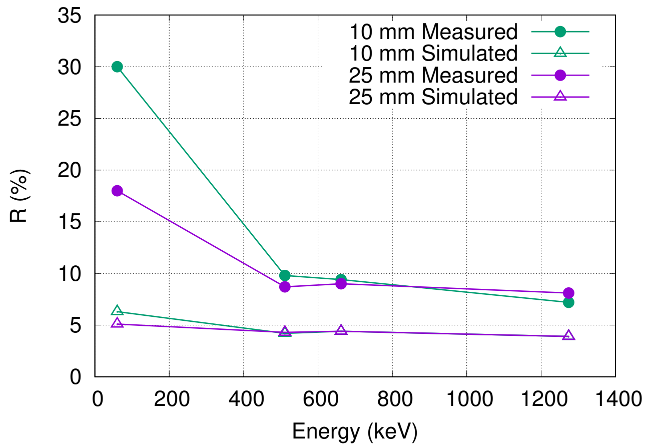

Figure 4. Measured and simulated energy resolution, as a function of the full-energy peak for 10 mm and 25 mm $CeBr_3$ scintillators.

3.2 Position resolution

Previously, multi-anode photomultiplier position resolution was studied by our team [8]. There, a plastic scintillator was coupled to multi-anode PMT [23] and scanned with electrons from ^{90}Sr/^{90}Y source. Position resolution better than 8 mm was obtained. This set-up was used to emulate a gamma detector comprising thin scintillator and position-sensitive photo-sensor in which, after the first scattering, the scattered gamma-ray leaves the detector volume. What would be left inside the crystal are electrons with continuous spectrum that will depend on the incident gamma-ray energy, which is exactly the case of thin crystal where single compton scattering event takes place.

Here we present preliminary results for position resolution shown in figure 5, from Geant4 simulation of $CeBr_3$ detector response when irradiated with gamma-rays. The simulation used 25 mm thick $CeBr_3$ scintillator coupled to 256 channel multi-anode PMT with pixel size 2.8 by

2020 JINST 15 C01013

2.8 mm^2 [23]. The contributions to the reconstructed position resolution are the unknown point of the interaction of the gamma-ray along its path through the scintillator, the photocollection, and the reflection properties of the surfaces for the used crystal. The reflection properties include whether the coverage provides diffuse or straight reflection, the uniformity of the coverage, and the reflection coefficient.

Despite the thickness of the crystal (25 mm), its position resolution is approximately 5.3 by 5.3 mm^2 (2σ) as obtained by the simulations with fixed gamma-rays energy at 662 keV, shown in figure 5.

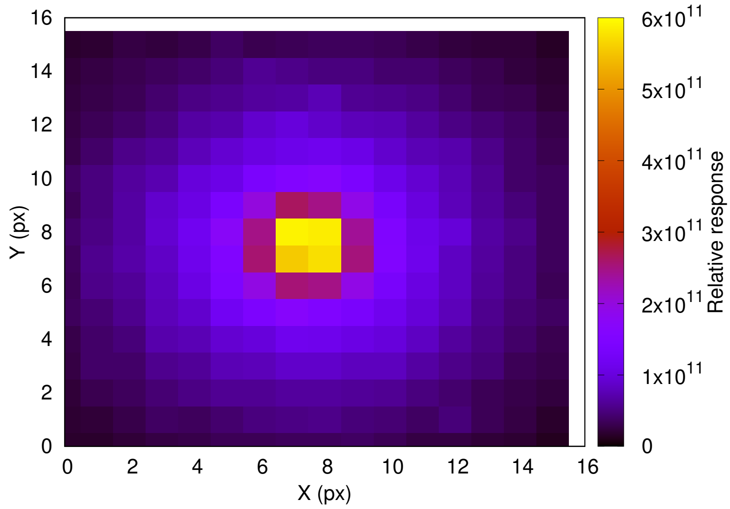

Figure 5. Distribution of incident photons, E_γ = 662 keV, on the transparent surface of the photomultiplier made with Geant4 simulations for 25 mm thick $CeBr_3$ detector.

4 Conclusion and outlook

Research and development of $CeBr_3$-based detectors is now being carried out at the University of Sofia. Studies of the energy resolution of $CeBr_3$ scintillators with two different thicknesses are presented. These crystals are suitable for development of a position-sensitive scintillation detectors for space-borne nano-telescopes. The poor energy resolution of the $CeBr_3$ crystals obtained in these measurements are caused by incomplete light collection by the PMT. This effect is more prominent for the thinner crystal at low energies. It is rather attributed to the geometry of the set up.

This work reports also on preliminary results from Geant4 simulations for the position resolution. The scintillation light from a monolithic $CeBr_3$ was assumed to be detected by a 2.8×2.8 mm^2 segmented photodetector. The simulations performed by the group show that good position resolution can be obtained even for 25 mm thick $CeBr_3$ crystals, which is in line with the working hypothesis. The presented results confirm that a scintillation detector coupled to a position-sensitive photodetector can fulfill the needs of gamma-ray astronomy on the performance side.

The readout electronics of the proposed Compton camera has to provide both time and amplitude/charge measurements. The time measurement will allow to precisely determine the coincidence between the two scintillation detectors and diminish the background due to accidental

2020 JINST 15 C01013

activity. The amplitude measurement of each individual channel will allow the determination of the center of gravity of the scintillation light pulse giving the position with the desired resolution. While in principle such measurements are regularly done with laboratory equipment further work is ongoing to demonstrate and develop sufficiently compact and cost effective solution suitable for space-based applications.

Acknowledgments

This work is supported by the Bulgarian National Science Fund under contract number DN18/17.

References

[1] S. Aldawood et al., *Development of a Compton camera for prompt-γ medical imaging*, *Rad. Phys. Chem.* **140** (2017) 190.

[2] V. Schonfelder, *The universe in gamma rays*, Springer, Germany (2001).

[3] ESA, *INTEGRAL*, https://sci.esa.int/web/integral.

[4] A. De Angelis et al., *Science with e-Astrogam*, *JHEA* **19** (2018) 1 [arXiv:1711.01265].

[5] A. Moiseev, *Compton-Pair production space telescope (ComPair) for MeV gamma-ray astronomy*, arXiv:1508.07349v2.

[6] Sean Griffin, *Subsystem Development for the All-Sky Medium Energy Gamma-ray Observatory (AMEGO) prototype*, talk given at the 36$^{\text{th}}$ *International Cosmic Ray Conference (ICRC2019)*, July 24–August 1, Madison, U.S.A. (2019), arXiv:1908.04154.

[7] NASA, *COMPTEL*, https://heasarc.gsfc.nasa.gov/docs/cgro/comptel/.

[8] Zh. Toneva et al., *Research and Development of a position-sensitive scintillator detector for γ- and X-ray imaging and spectroscopy*, in *Basic Concepts in Nuclear Physics: Theory, Experiments and Applications (RABIDA 2018)*, J.E. Garcia-Ramos et al. eds., Springer Proceedings in Physics volume 225, Springer, Germany (2019).

[9] NASA, *3D resources, CubeSat*, https://nasa3d.arc.nasa.gov/detail/cubesat.

[10] F.G.A. Quarati et al., *Scintillation and detection characteristics of high-sensitivity $CeBr_3$ γ-ray spectrometers*, *Nucl. Instrum. Meth.* **A 729** (2013) 596.

[11] S. Lo Meo et al., *Optical physics of scintillation imagers by Geant4 simulations*, *Nucl. Instrum. Meth.* **A 607** (2009) 259.

[12] A. Gostojic et al., *Characterization of $LaBr_3$:Ce and $CeBr_3$ calorimeter modules for 3D imaging in gamma-ray astronomy*, *Nucl. Instrum. Meth.* **A 832** (2016) 24.

[13] L.M. Fraile et al., *Fast timing study of a $CeBr_3$ crystal: time resolution below 120 ps at ^{60}Co energies*, *Nucl. Instrum. Meth.* **A 701** (2013) 235.

[14] M. Moszynski et al., *New photonics XP20D0 photomultiplier for fast timing in nuclear medicine*, *Nucl. Instrum. Meth.* **A 567** (2006) 31.

[15] A. Ulyanov et al., *Localisation of gamma-ray interaction points in thick monolithic $CeBr_3$ and $LaBr_3$:Ce scintillators*, *Nucl. Instrum. Meth.* **A 844** (2017) 81.

[16] HZC photonics, *Phoromultiplier tubes product manual*, http://www.hzcphotonics.com/products/ProductManual.pdf.

[17] CAEN electronic instrumentation, *User manual UM3350*, http://www.caen.it/csite/CaenProd.jsp?idmod=602&parent=11.

[18] ORTEC, *Model 113 scintillation preamplifier operating and service manual*.

[19] ORTEC, *Model 671 spectroscopy amplifier operating and service manual*.

[20] CAEN, *Technical information manual 8KMOD. N957 multichannel analyzer*.

[21] GEANT4 collaboration, *Geant4 — A simulation toolkit*, *Nucl. Instrum. Meth.* **A 506** (2003) 250.

[22] Z.S. Hartwig and P. Gumplinger, *Simulating response functions and pulse shape discrimination for organic scintillation detectors with Geant4*, *Nucl. Instrum. Meth.* **A 737** (2014) 155.

[23] Hamamatsu Photonics, *Flat panel type multianode photomultiplier tube assembly H9500, H9500-03*, http://www.hamamatsu.com/eu/en/product/category/3100/3002/H9500/index.html.

[24] GEANT4 collaboration, *GDML user's guide*, http://lcgapp.cern.ch/project/simu/framework/GDML/doc/GDMLmanual.pdf.

2020 JINST 15 C01013